Indian J. Phys. **51A**, 262-269 (1977)

Excitation of multilayered cylindrical structures with the help of ring source

SUBHAS CHANDRA SHARMA* AND J. S. VERMA

Department of Physics, Birla Institute of Technology and Science, Pilani Rajasthan

(*Received* 18 *February* 1976, *revised* 27 *May* 1976)

A cylindrical geometry consisting of a conductor (radius a_1), ring source (radius a), aircolumn (radius b) thin layer of Sb (radius c), thin layer of superconductor (radius d) and a thin layer of Sb (radius e such that $a_1 < a < b < c < d < e$) is studied. The ring source is assumed to be the ring of magnetic currents. This structure gives the multiple peaks of radiation field of equal magnitude at different angles including some peaks of less radiation field at other angles for different values of various parameters of this structure

1. INTRODUCTION

Source excitation of cylindrical structure has been studied by Sharma *et al* (1975) and Ram Chandra *et al* (1974). In addition to this multilayered transmission lines are also investigated by Dmitriyev *et al* (1973). Here in this article we intend to discuss the radiation pattern of the multilayered system while exciting with the help of ring of magnetic currents. The ring source is assumed to be situated in air. The air column is surrounded by thin layers of antimony, superconductor and antimony. The geometry consists of a conductor along its z axis. The radius of conductor, ring source, air column antimony layer, superconductor and outer antimony layer are respectively a_1, a, b, c, d and e $(a_1 < a < b < c < d < e)$.

2. ANALYSIS

The ring source is situated in $z = 0$ plane. The source term is given by $M = \hat{\phi}\,\delta(z)\,\delta(\rho - a)$ Where $\hat{\phi}$ is the unit vector along ϕ direction of the cylindrical coordinates and δ being the Kronecker's delta function. Following the procedure given by Dhani Ram *et al* (1972) one can arrive at the following solutions for the first asymmetric mode in cylindrical coordinates.

$$h_1 = A_1J_1(v_0\rho)+B_1Y_1(v_0\rho)\quad a_1 < \rho < a \qquad \dots \quad (1a)$$
$$h_2 = A_2J_1(v_0\rho)+B_2Y_1(v_0\rho)\quad a < \rho < b \qquad \dots \quad (1b)$$
$$h_3 = A_3J_1(v_1\rho)+B_3Y_1(v_1\rho)\quad b < \rho < c \qquad \dots \quad (1c)$$
$$h_4 = A_4J_1(v_2\rho)+B_4Y_1(v_2\rho)\quad c < \rho < d \qquad \dots \quad (1d)$$
$$h_5 = A_5J_1(v_1\rho)+B_5Y_1(v_1\rho)\quad d < \rho < e \qquad \dots \quad (1e)$$
$$h_6 = A_6H_1^{(1)}(v_0\rho)\quad e < \rho \qquad \dots \quad (1f)$$

---

* Present address : Department of Physics, M. M. College, Modinagar–201204.

Where h is the Fourier's Transform of H_φ given by

$$h(\rho, k_z) = \int_{-\infty}^{\infty} H_\varphi(\rho, z) e^{-jk_z z} dz$$

and the inverse transform is given by

$$H_\varphi(\rho, z) = \frac{1}{2\pi} \int_{-\infty}^{\infty} h(\rho, k_z) e^{jk_z z} dk_z$$

J_n, Y_n, and $H_n^{(1)}$ are Bessel functions of first kind, second kind and Hankel function of first kind respectively of n-th order

$$v_0^2 = w^2\mu_0\epsilon_0 - k_z^2$$

$$v_1^2 = w^2\mu_0\epsilon_0\epsilon_a - k_z^2$$

and $$v_2^2 = w^2\mu_0\epsilon_a\epsilon_s - k_z^2$$

where w, μ_0, ϵ_0, ϵ_a and ϵ_s are respectively the source frequency, permeability and permittivity of free space, propagation vector, dielectric constant for antimony layer and dielectric constant for superconductor

Now applying the following boundary conditions

(i) At $\rho = a_1$, the tangential electric vector viz $E_z(\rho, z)$ is continuous. Therefore

$$\left.\frac{dh_1}{d\rho} + \frac{h_1}{\rho}\right|_{\rho = a_1 + \delta} = 0$$

(ii) At the location of the magnetic ring source of electromagnetic waves ($\rho = a$) the continuation of H_φ and jump conditions gives

$$h_1|_{a-\delta} = h_2|_{a+\delta}$$

$$\left.\frac{dh_2}{d\rho}\right|_{a+\delta} - \left.\frac{dh_1}{d\rho}\right|_{a-\delta} = -jw\epsilon_p$$

(iii) At $\rho = b$, the continuation of H_φ and E_z will give

$$h_2|_{b-\delta} = h_3|_{b+\delta}$$

$$\epsilon_a \left.\left(\frac{dh_2}{d\rho} + \frac{h_2}{\rho}\right)\right|_{b-\delta} = \left.\left(\frac{dh_3}{d\rho} + \frac{h_3}{\rho}\right)\right|_{\rho = b+\delta}$$

(iv) At $\rho = c$, the continuation of H_φ and E_z will give

$$h_3|_{c-\delta} = h_4|_{c+\delta}, \quad \frac{\epsilon_s}{\epsilon_a} \left.\left(\frac{dh_3}{d\rho} + \frac{h_3}{\rho}\right)\right|_{c-\delta} = \left.\left(\frac{dh_4}{d\rho} + \frac{h_4}{\rho}\right)\right|_{c+\delta}$$

(v) Again at $\rho = d$, the continuation of H_φ and E_z will give

$$h_4|_{d-\delta} = h_5|_{d+\delta} \quad \frac{\epsilon_a}{\epsilon_s}\left|\frac{dh_4}{d\rho}+\frac{h_4}{\rho}\right|_{d-\delta} = \left|\frac{dh_5}{d\rho}+\frac{h_5}{\rho}\right|_{d+\delta}$$

(vi) At $\rho = e$, the continuation of H_φ and E_z will give

$$h_5|_{e-\delta} = h_6|_{e+\delta}, \quad \left|\frac{dh_5}{d\rho}+\frac{h_5}{\rho}\right|_{e-\delta} = \epsilon_a\left|\frac{dh_6}{d\rho}+\frac{h_6}{\rho}\right|_{e+\delta}$$

where $\delta \to 0$

After applying these boundary conditions one can get the magnitude of A_6 occurring in eq. (1f)

Now in $e < \rho$ region

$$H_\varphi = \frac{1}{2\pi}\int_{-\infty}^{\infty} A_6 H_1^{(1)}(V_0\rho)\exp(jk_z z)dk_z \quad \ldots \quad (2)$$

The variables (v_0, v_1 and v_2) occurring in this eq. have multiple values in the neighbourhood of $v_0 = 0$, $v_1 = 0$ and $v_2 = 0$ respectively. The integrand happens to be even function of k_z when one expands it about $v_0 = 0$. But Hankel's function appearing in the integrand has logarithmic singularity and hence gives branch points of the integrand. Considering the eq. (2) to be evaluated in k_z plane as contour integral. Introduce the transofrmation

$$k_z = k_0 \sin\tau$$

where $\tau = \lambda + j\alpha$

This transforms the region of integration in k_z plane into a strip of τ plane, which is bounded by two curved lines corresponding to the branch cuts $k = \pm k_0$ in τ plane. The branch cuts in τ plane are given by

$$\sin\lambda \cosh\alpha = \pm 1$$

which yields

$$V_0 = k_0\cos\tau, \qquad V_1 = k_0\sqrt{(\epsilon_a - \sin^2\tau)} \quad \text{and}$$

$$V_2 = k_0\sqrt{(\epsilon_s - \sin^2\tau)}$$

and eq. (2) gets transformed to

$$H_\varphi(\rho, z) = \frac{1}{2\pi}\int A_6(\tau)H_1^{(1)}(k_0\rho\cos\tau)\exp(jk_0\sin\tau)k_0\cos\tau d\tau \quad \ldots \quad (3)$$

Shifting from cylindrical coordinates (ρ, ϕ, z) to spherical coordinates (r, θ, ϕ) and taking approximate value of Hankel function of the integrand of eq (3) for large values of r, we have

$$H_\phi(r, z)\frac{1}{2\pi} \int A_6(\tau) \exp(-3\pi j/4)\left[\frac{2}{\pi k_0 r \cos\theta \cos\tau}\right]^{\frac{1}{2}} \times$$

$$\exp[jk_0 r \cos(\tau-\theta)]k_0 \cos\tau d\tau \quad .. \quad (4)$$

Saddle point of eq. (4) is given by

$$\frac{d}{d\tau}\cos(\tau-\theta) = 0$$

which gives $\tau = \theta$ saddle point.

The steepest Descent Path is given by the constant phase of exponential factor of the integrand of eq (4) and is to pass through the saddle point. So one can have

$$Im\, j \cos(\tau-\theta) = \text{const}$$

and is pass through $\tau = \theta$ which gives

$$\cos(\lambda-\theta)\cos h\alpha = 1$$

$$\sin(\lambda+\pi/2-\theta)\cos h\alpha = 1$$

This is plotted in the Fig 1 Now taking the help from standard method

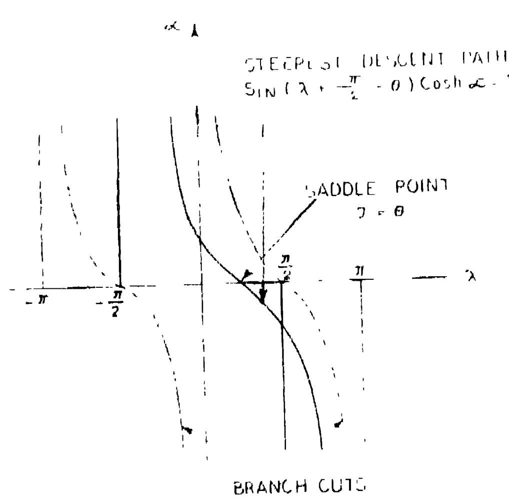

Fig. 1. τ plane representation for saddle point method

(Collin, 1960) for the lowest order approximation of the integral, one can end up with

$$H_\phi(r,\theta) = \frac{j\omega a}{2\pi} F(\theta) \frac{e^{-jk_0 r}}{r},$$

Here $F(\theta) = |A_6(k_z = k_0 \sin\theta)|$ and

A_6 is given by

$$A_6 = \frac{R_{74}(R_{78}-R_{76})}{R_{78}R_{75}-R_{77}R_{76}}$$

$$\begin{aligned}
R_{71} = {} & [\{\epsilon_a V_2 Y_1(v_2 d) J_1(v_2 d) - \epsilon_a V_2 Y_0(v_2 d) J_1(v_2 d)\}\{Y_1(v_2 d)\{\epsilon_a V_2 J_0(V_2 c) Y_1(v_1 c) \\
& - J_1(v_2 c)\epsilon_s V_1 Y_0(v_1 c)\}\{J_0(v_1 c) Y_1(v_1 c) - Y_0(v_1 c) J_1(v_1 c)\}\epsilon_s V_1 - \{J_1(v_2 c)\epsilon_s V_1 J_0(v_1 c) \\
& - \epsilon_a V_2 J_0(v_2 c) J_1(v_1 c)\} Y_1(v_2 d) R_{57} - J_1(v_2 d)\{\epsilon_a V_2 Y_0(v_2 c) Y_1(v_1 c) \\
& - \epsilon_s V_1 Y_0(v_1 c) Y_1(v_2 c)\}\{J_0(v_1 c) Y_1(v_1 c) - Y_0(v_1 c) J_1(v_1 c)\}\epsilon_s V_1 \\
& - \{Y_1(v_2 c)\epsilon_s v_1 J_0(v_1 c) - \epsilon_a V_2 Y_0(v_2 c) J_1(v_1 c)\} J_1(v_2 d) R_{57}] \\
& [\epsilon_s V_1\{J_0(v_1 c) Y_1(v_1 c) - Y_0(v_1 c) J_1(v_1 c)\}\{J_1(v_1 c)\epsilon_s v_1 Y_0(v_1 c) \\
& - \epsilon_a V_0 J_0(v_0 b) Y_1(v_1 c)\} Y_1(v_0 b)\Big[\frac{J_1(v_0 a) Y_0(v_0 a_1)}{J_0(v_0 a_1)}\{V_0 a J_0(v_0 a) - J_1(v_0 a) \\
& - v_0 a Y_0(v_0 a)\} - Y_1(v_0 a) - v_0 a\}\{J_0(v_0 a) Y_1(v_0 a) - J_1(v_0 a) Y_0(v_0 a)\}\} \\
& - \{J_1(v_1 b) v_0 a\{Y_0(v_0 a) J_1(v_0 a) - Y_1(v_0 a) J_0(v_0 a)\}\{v_0 a J_0(v_0 a) J_0(v_0 a) \\
& - J_1(v_0 a)\}\frac{Y_0(v_0 a_1)}{J_0(v_0 a_1)}\Big] - \left\{\begin{array}{l}\epsilon_a V_0 J_0(v_0 b) Y_0(v_0 b) - V_1 J_0(v_1 b) Y_1(v_0 b) \\ \epsilon_a V_0 Y_0(v_0 b)\}\{J_1(v_0 b) - \epsilon_a V_0 J_0(v_0 b)\}\end{array}\right\} \\
& [V_0 a Y_1(v_0 b)\{V_0 a J_0(v_0 a) - J_1(v_0 a)\}\{J_0(v_0 a) Y_1(v_0 a) - J_1(v_0 a) Y_0(v_0 a)\} \\
& - \frac{J_1(v_0 b) V_0 a Y_0(v_0 a_1)}{J_0(v_0 a_1)}\{Y_0(v_0 a) J_1(v_0 a) - Y_1(v_0 a) J_0(v_0 a)\}\{V_0 a J_0(v_0 a) - J_1(v_0 a)\}]
\end{aligned}$$

$$\begin{aligned}
R_{57} = {} & \{J_1(v_1 c)\epsilon_s V_1 Y_0(v_1 c) - \epsilon_a V_0 J_0(v_0 b) Y_1(v_1 c)\} Y_1(v_1 b)\frac{v_0 a Y_0(v_0 a_1)}{J_0(v_0 a_1)} \\
& \{Y_0(v_0 a) J_1(v_0 a) - Y_1(v_0 a) J_0(v_0 a)\}\{v_0 a J_0(v_0 a) - J_1(v_0 a)\} \\
& - \frac{J_1(v_1 b) v_0 a Y_0(v_0 a_1)}{J_0(v_0 a_1)}\{Y_0(v_0 a) J_1(v_0 a) - Y_1(v_0 a) J_0(v_0 a)\} \\
& \{v_0 a) J_0(v_0 a) - J_1(v_0 a)\} - \left[\begin{array}{l}\epsilon_a V_0 J_1(v_1 b) Y_0(v_0 b) - V_1 J_0(v_1 b) Y_1(v_0 b) \\ \epsilon_a V_0 Y_0(v_0 b)\}\{J_1(v_0 b) - \epsilon_a V_0 J_0(v_0 b)\}\end{array}\right] \\
& [v_0 a Y_1(v_0 b)\{v_0 a J_0(v_0 a) - J_1(v_0 a)\}\{J_0(v_0 a) Y_1(v_0 a) - J_1(v_0 a) Y_0(v_0 a)\} \\
& - \frac{J_1(v_0 b) v_0 a Y_0(v_0 a_1)}{J_0(v_0 a_1)}\{Y_0(v_0 a) J_1(v_0 a) - Y_1(v_0 a) J_0(v_0 a)\}\{v_0 a J_0(v_0 a) - J_1(v_0 a)\}]
\end{aligned}$$

$$\begin{aligned}
R_{72} = {} & -[\{\epsilon_s V_1 J_0(v_1 d) J_1(v_2 d) - \epsilon_a V_2 J_1(v_1 d) J_1(v_2 d)\}\{Y_1(v_2 d) R_{59} - J_1(v_2 d) R_{60}\} \\
& + R_{59} J_1(v_1 d)\{Y_1(v_2 d)\epsilon_a V_2 J_1(v_2 d) - \epsilon_a V_2 Y_0(v_2 d) J_1(v_2 d)\}]
\end{aligned}$$

$$R_{59} = \{c_a V_2 J_0(v_2c) Y_1(v_1c) - J_1(v_2c) c_s V_1 Y_0(v_1c)\}\{J_0(v_1c) Y_1(v_1c) - Y_0(v_1c) J_1(v_1c)\} c_s V_1 - \{J_1(v_2c) c_s V_1 J_0(v_1c) - c_a V_2 J_0(v_2c) J_1(v_1c)\} R_{57}$$

$$R_{60} = \{c_a V_2 Y_0(v_2c) Y_1(v_1c) - c_s V_1 Y_0(v_1c) Y_1(v_2c)\}\{J_0(v_1c) Y_1(v_1c) - Y_0(v_1c) J_1(v_1c)\} c_s V_1 - \{Y_1(v_2c) c_s V_1 J_0(v_1c) - c_a V_2 Y_0(v_2c) J_1(v_1c)\} R_{57}$$

$$R_{75} = \frac{H_1(v_0c)}{J_1(v_1c)} R_{72}$$

$$R_{73} = \{c_s V_1 Y_0(v_1d) J_1(v_2d) - c_a V_2 Y_1(v_1d) J_1(v_2d)\}\{Y_1(v_2d) R_{59} - R_{60} J_1(v_2d)\} + \{Y_1(v_2d) c_a V_2 J_1(v_2d) - c_a V_2 Y_0(v_2d) J_1(v_2d)\}\{R_{59} Y_1(v_1d)\}$$

$$R_{76} = R_{73} - \frac{Y_1(v_1c)}{J_1(v_1c)} R_{72}$$

$$R_{77} = \frac{c_a V_0 H_0(v_0c)}{v_1 J_0(v_1c)} R_{72}$$

$$R_{78} = R_{73} - R_{72} \frac{Y_0(v_1c)}{J_0(v_1c)}$$

By varying various parameters occurring in expression of A_ϕ one can get the characteristics of the radiation field.

3. Results and Conclusion

The value of $|A_\phi|$ was computed with the help of IBM-1130 computer for various values of parameters given by c_a and $c_s (\gamma_0 = 10^{-12}, \lambda_0 = 500 \times 10^{-8}, t = 0.1, k = \omega/c)$. The computed results are given in table 1 and also plotted

Table 1. Effect of the radius of the ring source (a)
$a_1 = 0.1$ cm, $b = 2.8$ cm, $c = 2.80005$ cm, $d = 2.800055$ cm, $e = 2.800105$, $\omega = 2\pi \times 10^{15}$ rad sec^{-1}, $a = 2.0$ cm

The direction (in degrees) given below have less intense radiation field (in relative units). The directions other than these have the maximum amplitude of the radiation field (in relative units having value 1.1421356)

72.50, 15.25, 12.75, 7.75, 48.25, 14.25, 25.25, 24.0, 31.0, 18.0, 23.50, 75.5, 19.25, 47.5, 7.0, 44.0, 18.25, 17.25, 15.5, 36.75, 15.0, 59.5, 17.5, 2.0, 1.5, 2.25, 1.25, 1.0, 24.25, 2.5, 0.75, 5.0, 17.5, 0.5, 0.25, 73.74, 2.75, 14.75, 24.5, 42.75, 3.0, 4.5, 12.5, 43.0, 1.75, 31.50, 25.75, 4.25, 3.25, 37.25, 38.0, 16.0, 31.25, 30.25, 17.0, 76.25, 32.0, 19.25, 67.0, 54.25, 3.5, 4.0, 60.25, 37.5, 16.25, 41.5, 15.75, 3.75, 90.0, 30.50, 8.0, 48.5, 51.0, 19.0, 5.75, 54.75, 24.75, 25.0, 16.5, 23.75, 8.25, 42.0, 17.25, 18.75, 31.75, 26.0, 26.75, 11.5, 16.75

These directions have the magnitude of the radiation field respectively

1.3923, 1.3535, 1.3425, 1.3050, 1.2806, 1.2719, 1.2627, 1.2114, 1.1960, 1.1799, 1.1778, 1.1655, 1.1533, 1.1443, 1.1285, 1.1206, 1.1102, 1.0891, 1.0819, 1.0694, 1.0683, 1.0636, 1.0622, 1.0615, 1.0586, 1.0547, 1.0525, 1.0456, 1.0451, 1.0424, 1.0395, 1.0376, 1.0366, 1.0349, 1.0320, 1.0284, 1.0269, 1.0198, 1.0178, 1.0137, 1.0129, 1.0113, 1.0105, 1.0067, 1.063, 1.0049, 1.0042, 1.0036, 1.0034, 1.0028, 1.0022, 1.0018, 1.0016, 1.0015, 1.0014, 1.0007, 1.0007, 1.0003, 1.0002, 1.0002, 1.0001, 1.0, 1.0, 1.0, 0.9833, 0.9146, 0.8735, 0.8676, 0.6889, 0.6825, 0.6635, 0.6503, 0.5502, 0.5193, 0.4945, 0.4022, 0.3173, 0.2302, 0.2213, 0.2029, 0.1353, 0.0986, 0.0918, 0.0798, 0.0743, 0.0743, 0.0282, 0.0188, 0.0005.

in the fig. 2. The plot shows the effect of the radius of the central conductor on radiation pattern. For having more precision in direction the plot is made only for first 10 degrees. This is a fraction of the total radiation pattern but this surely exhibits the general behaviour of the radiation field For $a_1 = 0.1$ *cm*

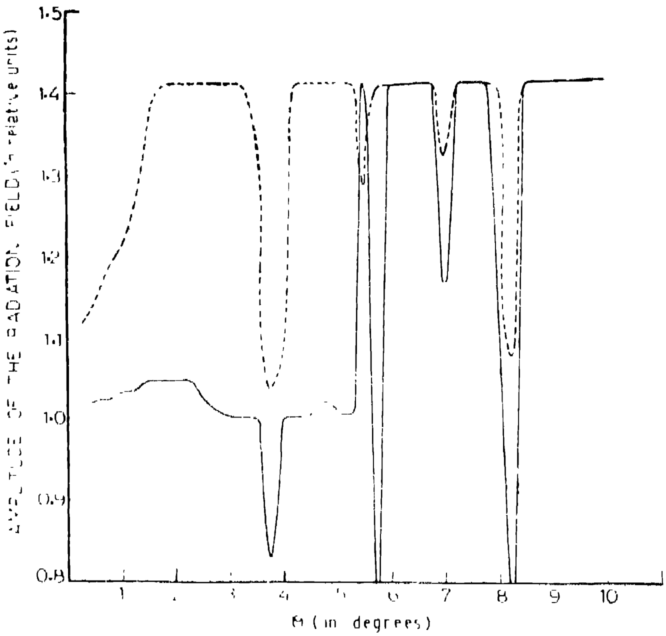

Fig 2. Variation of the field amplitude with direction fc

--- solid curve a_1 0.1 cm, } a = 1.85 cm, b = 2.8 cm, c = 2.80005 cm

- - - dotted curve a_1 = 0.15 cm } d = 2.800055 cm, 2.800105 cm w = $2\pi \times 10^{12}$ radsec^{-1}

(solid plot) it shows less broad maximum radiation zone while for a_1 = 0.15 cm (dotted line) there occurs five broad radiation zones having maximum radiation (1.75° to 3.25°, 4.25° to 5.25° to 6.75°, 7.25° to 8.0° and beyond 8.0°). This is of course a small range of direction but it is obvious when one proceeds towards higher θ the maximum radiation zone gets broadened and from 80° to 89.75° (for a_1 = 0.1 cm and a_1 = 0.15 cm) there occurs a uniform radiation zone having maximum radiation. But the direction of 90° remains to be having less intense radiation in all the cases The increase in a causes the more directions having less intense field (table 1) The variation in pattern due to the variation in other parameters is not reported here. This structure essentially gives the broad multi-peaks while on excitation with the help of ring source It is worth noticing that these results are obtained with the help of theoretical background and need to be verified experimentally. As far as the physical explanations are concerned the leaky waves excitation on such surface are the well proved phenomenon and hence the explanation rendered by Tamir *et al* (1962, 1963) seems to be most promising and acceptable. This radiation system can be visualized as multi-layered multipeak radiating system.

ACKNOWLEDGMENT

The author (SCS) is greatly indebted to CSIR (India) for providing him the research fellowship. It gives the pleasure to the authors to thank Dr. Ram Chandra also for constructive discussions on the subject matter of this article. The authors also wish to thank the referee for taking interest in making the valuable comments about the paper The help from IPC Staff of the Institute in computational work is also acknowledged with thanks

REFERENCES

Collin, 1960, *Field Theory of Guided Waves* (McGraw Hill Book Co.) p 195

Dhani Ram & Verma J S 1972 *Indian J. Pure and Appl. Phys.* **10**, 716.

Dmitriyev V. M & Prokopchenko A I 1973 *Radio Engineering and Electronic Physics* **16**, 1593.

Ram Chandra & Verma J. S. 1974 *Indian J Pure and Appl Physics* **12**, 192

Sharma Subhash Chandra, Ram Chandra & Verma J. S. 1975 *Ind. J. Pre. and Appl. Phys* **13**, 829

Sharma Subhash Chandra & Verma J. S. 1975 *Ind. J. Radio and Space Physics* **4**, 282.

Tamir, T. & Oliner A. A. 1962 *IRE Trans Anthenna Propag.* AP-10, 55

Tamir, T. & Oliner A. A 1963 *Proc. I E.E* **110**, 325.